Analysis of Optical Fiber Acoustic Transducer with a MEMS Membrane

Li Xiaolong Wang Jiang'an Zong Siguang

(*Electronic Engineering Institute, Naval University of Engineering, Wuhan, Hubei* 430033, *China*)

Abstract To be used in sound sensor field, a new intensity modulated optic microphone theory is introduced. Here single-mode optical fiber and single fiber C-lens are used to realize light intensity modulation; the system also contains micro-electro-mechanical system (MEMS) membrane to be compatible with vibration displacement. Simulation results show that the proper choice of parameters like membrane size can make the sensitivity of sensor improve in orders of magnitude than traditional light intensity modulation methods, and the experimental results also show that the theoretical simulation is persuasive.

Key words fiber optics; acoustic transducer; C-lens collimator; micro-electro-mechanical system

OCIS codes 060.2310; 040.1880; 230.0230

基于 MEMS 膜片的光纤声传感器分析

李晓龙 王江安 宗思光

(海军工程大学电子工程学院, 湖北 武汉 430033)

摘要 提出了一种新的应用于低频声传感领域的强度调制型光纤传感器理论模型。该模型使用了单模光纤来传输和接收光信号,使用了 C-lens 光学透镜实现光准直作用,讨论了光在准直透镜中的传播规律,利用准直器耦合损耗相对角度变化最为敏感的特征实现光强调制。强度型光纤传感器采用微电机系统(MEMS)结构的压力振动膜片拾取振动位移,通过分析施加在膜片上压力的变化得到影响光纤低频声传感器灵敏度的相关参数。仿真结果表明,选择合适的参数可以使传感器的灵敏度较传统方法有量级的提高,实验结果也说明了理论建模的可行性。

关键词 光纤光学;声传感器;C-lens 准直器;微电机系统

中图分类号 TN918.13 **文献标识码** A **doi**: 10.3788/CJL201340.1005007

1 Introduction

The technology is showing promise in the fields of industrial and environmental sensing before fiber optics, and the interest on fiber-optic microphones is also quickly growing because of the advantages that an optical sensor has over conventional sensors. These advantages include electrical and chemical passiveness and immunity to electromagnetic interference[1]. In addition, long distances between the microphone and the electronic circuit are supported due to the low loss, anti-electromagnetism interference, safety, and reliable characteristic of optical fiber. We can make full use of excellent characteristics of fiber-optic technology to pressure sensor, medicine, robotics, surveillance and so on[2-4].

For application of a reflective intensity modulation type fiber optic microphone (RIM-FOM), its reflective intensity modulation model is a critical and important step for improving its sensitivity performance. For example, based on the development of the existing model, some of the previously proposed solutions have analyzed the influence of the system geometry parameters on performance, and they have optimized the structure[5].

In this paper, coupling-loss formula about single-mode fiber (SMF) with C-lens is used. Micro-electro-mechanical system (MEMS) membrane used here can be subjected to deformation induced by acoustic wave.

收稿日期: 2013-05-29; **收到修改稿日期**: 2013-06-24

基金项目: 国家自然科学基金(51109217)

作者简介: 李晓龙(1985—),男,博士研究生,主要从事水下声光传感方面的研究。E-mail: lxl_3515@126.com

导师简介: 王江安(1951—),男,教授,博士生导师,主要从事光电技术方面的研究。E-mail: gdyfzx@163.com

MEMS deformation change leads to reflection light (the light will be reflected to C-lens) angular tilt change. The slight change of angular tilt can lead to significant change in optical coupling loss, which is the foundation of sensitivity.

This optical fiber sensing probe is different from the model of Song *et al.*[6], for which the structure seems complex and the cost of engineering applications will also be high. Another important difference is that the coupling efficiency of the light into the optical head is dependent upon the distance between the optical head and the diaphragm (Fig. 1 in Ref. [6]), and in view of calculating the overlap integral between the Gaussian beam profile of the lens and the beam reflected back from the diaphragm, this algorithm is similar with the model established by Sakamoto *et al.*[7]. The third difference is that the focus of Ref. [6] is only to find the initial operation point and its dynamic characteristics, while neither the sensitivity nor the specific numerical calculation related is given.

In addition, the simulation shows that the algorithm in this paper can not only improve the detection sensitivity of optical fiber sensing probe than traditional algorithm[8], but also solve the problem of practical application, which could be unrealistic for interference model[9] because of the complexity of demodulation structure. And experimental results also show that the establishment of this algorithm is feasible.

2 Optical coupling principle

Fiber-optic components such as single-mode fiber, wavelength-division multiplexers/de-multiplexers, circulators, switches, have become key devices for optical fiber sensing and optical fiber communications. This is because compared with conventional coupling model, the coupling between two fiber collimators has a large allowable separation distance with a low loss that is very important for free-space interconnected fiber-optic module or a practical optical fiber sensing subsystem.

Traditional coupling efficiency of two multimode fibers (MMFs) can be acquired by calculating the fractional overlap of two circles, the imaged spot of light and the mode field of the output fiber. When this method is adopted to single-mode fibers, the power density is changed to the Gaussian profile characteristic of the propagating fundamental mode, that is to say we should consider the Gaussian field approximation method to characterize the coupling loss[10-11] here, because separation misalignment, offset misalignment, angular misalignment and spot-size mismatch can all make coupling loss of fiber collimators change.

Acting variation pressures on fixed MEMS membrane can make the defection of membrane change, and obviously the relative position between SMF pigtailed fiber collimator and MEMS membrane will be changed too. The MEMS membrane has a highly flat, uniform surface featuring high optical reflectivity. The change of distance between collimator and flat membrane directly leads to the SMF pigtailed fiber collimator coupling loss. The compact optical head is shown in Fig. 1.

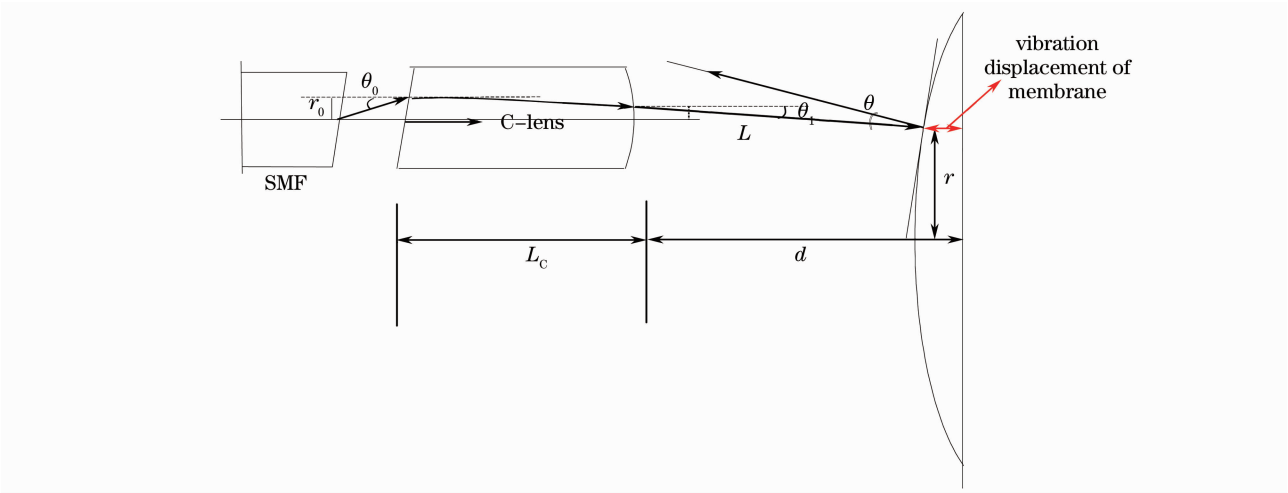

Fig. 1　Sensing probe in reflective fiber microphone.

3 SMF pigtailed fiber collimator coupling loss caused by MEMS membrane

3.1 Analysis about MEMS membrane design

For peripheral fixed supported round flat membrane, we assume that: the maximum deflection of membrane is smaller than a third thickness, using small deflection theory; acting uniform distributed static pressure on the membrane surface.

The deflection of flat membrane is defined as[12]

$$\omega = \frac{3p(1-\mu^2)}{16Eh^3}(R^2 - r^2)^2. \tag{1}$$

The lowest self-oscillation frequency of flat membrane is defined as

$$f_0 = \frac{10.17h}{2\pi R^2}\sqrt{\frac{E}{12(1-\mu^2)\rho}}. \tag{2}$$

In Eqs.(1) and (2), p is uniform pressure, h is flat membrane thickness, R is flat membrane radius, r is the radius distance from the central axis of flat membrane, μ is Poisson's ratio, E is elastic modulus, and ρ is the material's density of flat membrane.

MEMS flat membrane is etched in silicon base using micro processing technology. MEMS pressure sensor mainly consists of peripheral fixed supported round flat membrane, optical fiber collimating device, SMF, glass tube, etc. Figure 2 is the profile of the MEMS structure.

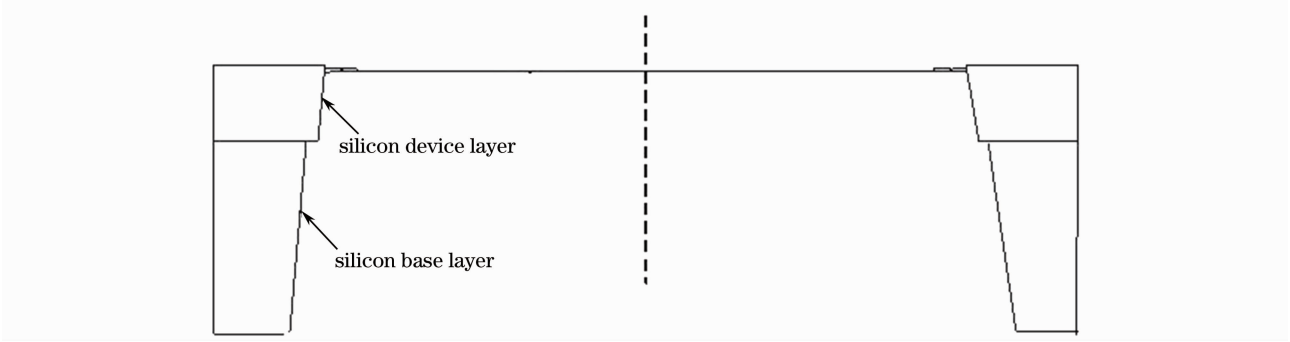

Fig.2 MEMS structure diagram.

3.2 Insertion loss analysis

We use C-lens as collimator lens. The C-lens has the ray matrix:

$$\boldsymbol{A}_1 = \begin{bmatrix} a & b \\ c & d \end{bmatrix} = \begin{bmatrix} 1 & L_C/n \\ (1-n)/R_1 & 1+(1-n)L_C/(nR_1) \end{bmatrix}, \tag{3}$$

where L_C is the length of C-lens, n is the refractive index of C-lens, R_1 is the radius of curvature. The Gaussian optical field emitted from C-lens has a modal field diameter of ω_1.

The x component of the Gaussian light-field vector in rectangular coordinate system can be expressed as

$$E_x(x,y,z) = E_1\frac{\omega_T}{\omega(z)}\exp\left\{-\mathrm{i}[kz-\eta(z)] - r^2\left[\frac{1}{\omega^2(z)} + \mathrm{i}\frac{k}{2R(z)}\right]\right\}, \tag{4}$$

where E_1 is the output field's amplitude at the origin position, ω_T is the Gaussian beam waist, $\eta(z) = \arctan\left(\frac{\lambda z}{\pi n\omega_T^2}\right)$.

The projection matrix inhomogeneous medium is $\boldsymbol{A}_2 = \begin{bmatrix} 1 & L \\ 0 & 1 \end{bmatrix}$, where L is the distance from the surface of C-lens to flat membrane, and $L = d - \frac{3p(1-\mu^2)}{16Eh^3}(R^2-r^2)^2$. The reflection matrix resulting from spherical reflector is $\boldsymbol{A}_3 = \begin{bmatrix} 1 & 0 \\ -\frac{2}{R_1} & 1 \end{bmatrix}$, where R_1 is the curvature radius of spherical reflector. Another projection matrix in homogeneous medium is $\boldsymbol{A}_4 = \begin{bmatrix} 1 & L/\cos\theta \\ 0 & 1 \end{bmatrix}$, where $L/\cos\theta$ is the reflected light distance from flat membrane to the surface of C-lens. Assume that the emitted light's coordinates are r_1, θ_1, and the received light's coordinates are r_2, θ_2.

Using the *ABCD* law, we have

$$\begin{bmatrix} r_1 \\ \theta_1 \end{bmatrix} = \boldsymbol{A}_1\begin{bmatrix} r_0 \\ \theta_0 \end{bmatrix} = \begin{bmatrix} a & b \\ c & d \end{bmatrix}\begin{bmatrix} r_0 \\ \theta_0 \end{bmatrix}, \tag{5}$$

$$\begin{bmatrix} r_2 \\ \theta_2 \end{bmatrix} = \boldsymbol{A}_4\boldsymbol{A}_3\boldsymbol{A}_2\begin{bmatrix} r_1 \\ \theta_1 \end{bmatrix} = \begin{bmatrix} a_1 & b_1 \\ c_1 & d_1 \end{bmatrix}\begin{bmatrix} r_1 \\ \theta_1 \end{bmatrix}. \tag{6}$$

Figure 3 shows three combined misalignments: X_0 is the offset misalignment between the longitudinal axes of the lenses; Z_0 is the separation misalignment between two lens surfaces; θ is the angular misalignment between the longitudinal axes of the lenses.

Because of the existence of pressure, peripheral fixed supported round flat membrane's displacement will be changed. Here coupling efficiency can be changed through affecting parameters like X_0, Z_0, θ. We can calculate X_0, Z_0, θ with $Z_0 = L + L/\cos\theta$, $X_0 = r_2 - r_1$, $\theta = |\theta_2| - |\theta_1|$.

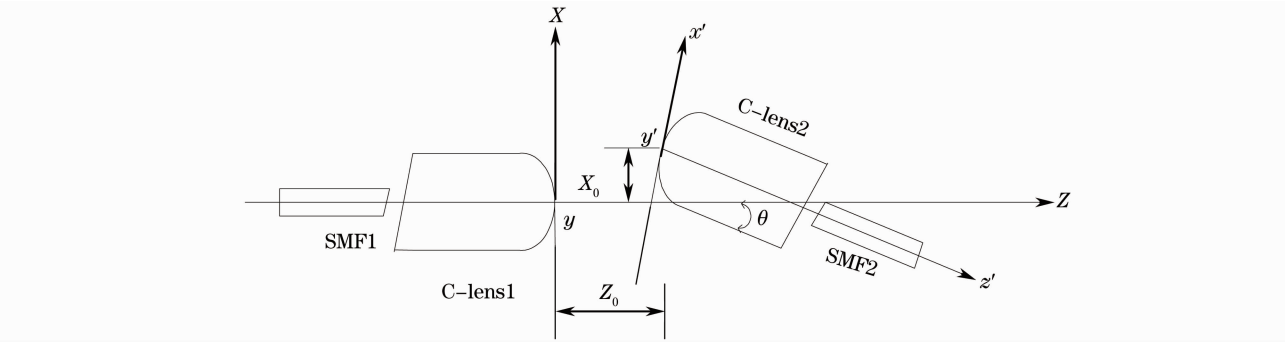

Fig. 3 Side view of two fiber collimators with three combined misalignments in two rectangular systems.

The coupling co-efficiency η_c at $z' = 0$ between two Gaussian beams can be expressed as[13-14]

$$\eta_c = \frac{2}{\pi E_1^2 \omega_T^2} \int_{-\infty-\infty}^{+\infty+\infty} E_x(x,y,z)\,|_{z'=0} \times E_{x'}^*(x',y',z')\,|_{z'=0}\,\mathrm{d}x'\mathrm{d}y'. \tag{7}$$

The power transmission coefficient can be written as $T = |\eta|^2 = \eta_c \eta_c^*$. We can calculate the power transmission coefficient T to be

$$T = 4\exp(-AC/B)D/B, \tag{8}$$

Where

$$A = (k\omega_T)^2/2,$$
$$B = G^2 + (D+1)^2,$$
$$C = (D+1)F^2 + 2DFG\sin\theta + D(G^2 + D + 1)\sin^2\theta,$$
$$D = (\omega_R/\omega_T)^2,$$
$$F = 2X_0/(k\omega_T^2),$$
$$G = 2Z_0/(k\omega_T^2),$$
$$k = 2\pi n/\lambda. \tag{9}$$

The total coupling loss in decibels between two misaligned (i. e., with three simultaneous misalignments) SMF collimators can be expressed as[15]

$$L_{tot}(X_0, Z_0, \theta) = -10\lg T = -10\lg\left[\frac{4D}{B}\exp\left(-\frac{AC}{B}\right)\right]. \tag{10}$$

Through these results we can calculate the sensitivity about coupling efficiency and the displacement of flat membrane.

4 SMF pigtailed fiber collimator coupling loss caused by MEMS membrane

When it is used at the 1.55 μm wavelength, the SMF has a 4.65 μm mode field radius. The air gap refractive index is 1. Poisson's ratio of the membrane $\mu = 0.3$, the thickness of flat membrane is h; the radius of flat membrane is R, elastic modulus of flat membrane $E = 1.7 \times 10^{11}$ Pa. The refractive index of C-lens is 1.7447, and the radius of curvature is 1.8 mm. The length of 1.5 mm is the initial interval between membrane and C-Lens. The location of outgoing beam from C-Lens is in its center, which is r (in μm) from the flat membrane axis.

Simulation curve of light intensity coupling loss is in following three cases. Figure 4 is the coupling loss curve when the thickness of membrane takes different values in condition of stable pressure of 5 Pa and flat membrane radius of 2.35 mm. Figure 5 is the coupling loss curve when the radius of membrane takes different values in condition of stable pressure of 5 Pa and flat membrane thickness of 4.75 μm. Figure 6 is the coupling loss curve when the displacement of membrane takes different values in condition of flat membrane radius of 2.35 mm and flat membrane thickness of 4.75 μm.

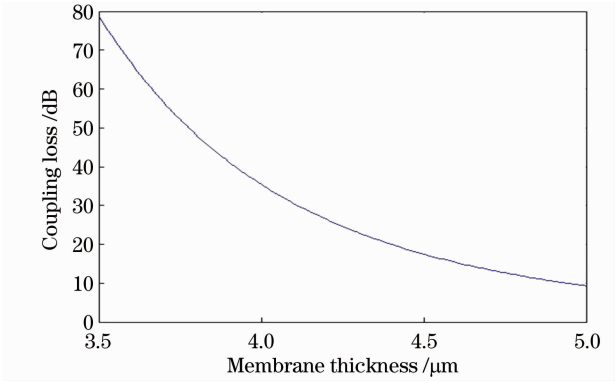

Fig. 4 Coupling loss curve when stable pressure is 5 Pa, flat membrane radius is 2.35 mm.

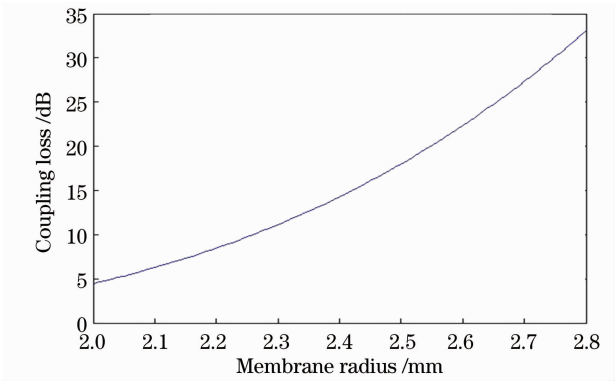

Fig. 5 Coupling loss curve when stable pressure is 5 Pa, flat membrane thickness is 4.75 μm.

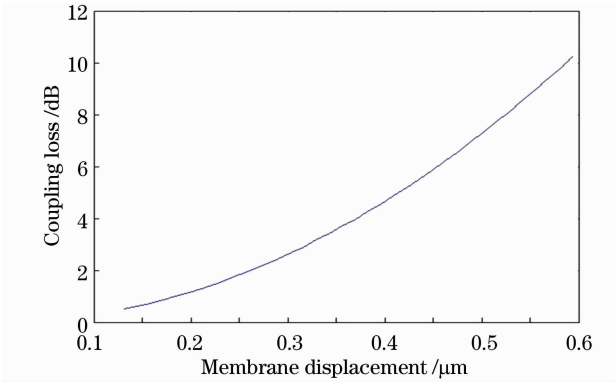

Fig. 6 Coupling loss curve of different displacement about flat membrane when its radius is 2.35 mm, thickness is 4.75 μm.

The displacement of flat membrane change leads to reflection light (the light will be reflected to C-lens) angular tilt change, and the change of angular title leads to optical coupling loss change. The greater the displacement change, the higher the coupling loss change, and the sensitivity therefore could be obtained.

The simulation results show that, in condition of fixed pressure acting on flat membrane, with the radius of flat membrane increasing, the displacement resulting from fixed pressure will be larger, so the coupling loss is increasing; with the thickness of flat membrane increasing, the displacement resulting from fixed pressure will be smaller, so the coupling loss is descending. In condition of the size of the flat membrane fixed, with the pressure acting on flat membrane increasing, the displacement resulting from fixed pressure will be larger, so the coupling loss is increasing. And the sensitivity is established on the basis of coupling loss, for a certain displacement change, the greater the coupling loss change, the higher the sensitivity obtained.

5 Experimental verification

To verify our theoretical results, we performed a series of measurements using the experimental setup shown in Fig. 7.

In our experiments, signal generator, loudspeaker, adjusting bracket, C-lens SMF, MEMS flat membrane, optical power meter andsingle spectrum light source were used. A diode laser at 1550 nm was employed as the light source, the SMF had a 9.3-μm mode field diameter (which indicates that ω_0 = 4.65 μm). The refractive index of C-lens was 1.7447, the air gap refractive index was 1, and the radius of curvature was 1.8 mm. The power of light source was 250 μW. The experimental device is shown is Fig. 8. From Fig. 8(b), we can see that when there is no pressure acting on the flat membrane the loss of Gaussian beam is 2.02 dB (considering the loss of circulator, instability of reference light, imperfection of C-lenses and back reflection of the lens surfaces). Figure 9 (a) is the elevation of MEMS sensitive diaphragm, and Fig. 9(b) is the back elevation of MEMS sensitive diaphragm. The MEMS sensitive diaphragm is round in a black wireframe. Because of the restriction of workmanship, to achieve good results, the radius of membrane was designed as 2.35 mm, and the thickness of flat membrane was designed as 7 μm. And what should be noted is that when the radius of membrane is fixed at 2.35 mm, the change of membrane thickness does not affect the simulation results of Fig. 6. Because the membrane thickness does not directly affect the coupling loss, even if the flat membrane thickness is 7 μm, if the membrane has the same vibration displacement, the coupling loss curve will be the same.

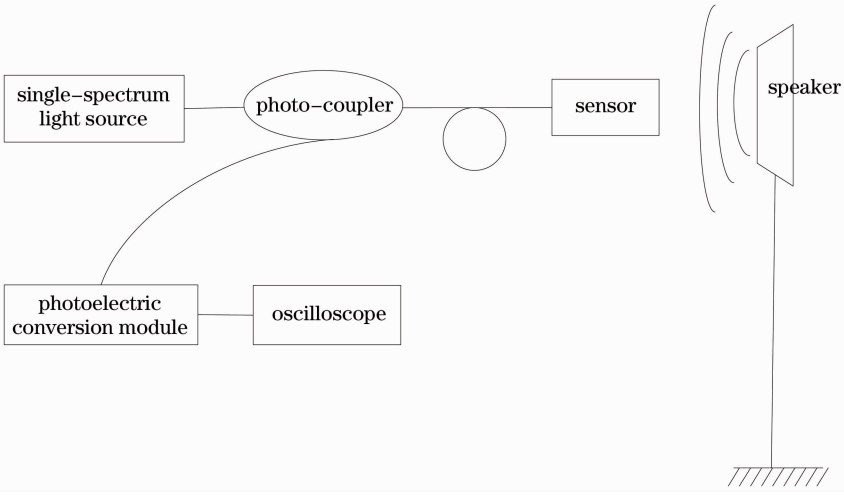

Fig. 7　Experimental setup

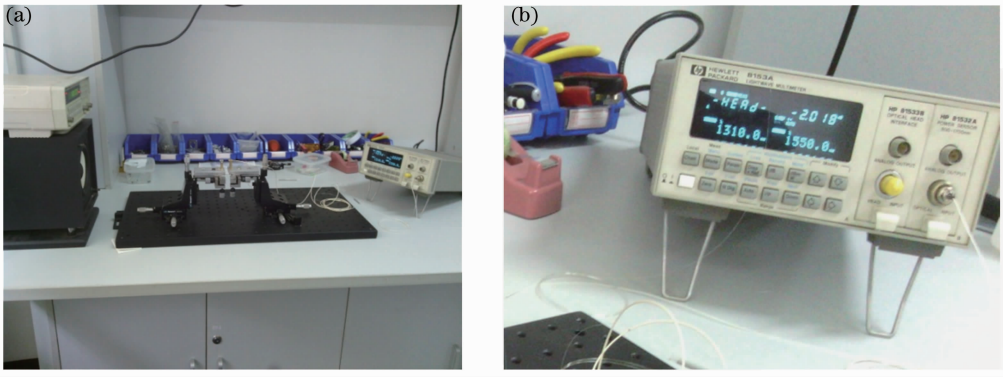

Fig. 8　Experimental device diagram. (a) Total sceme; (b) partial view

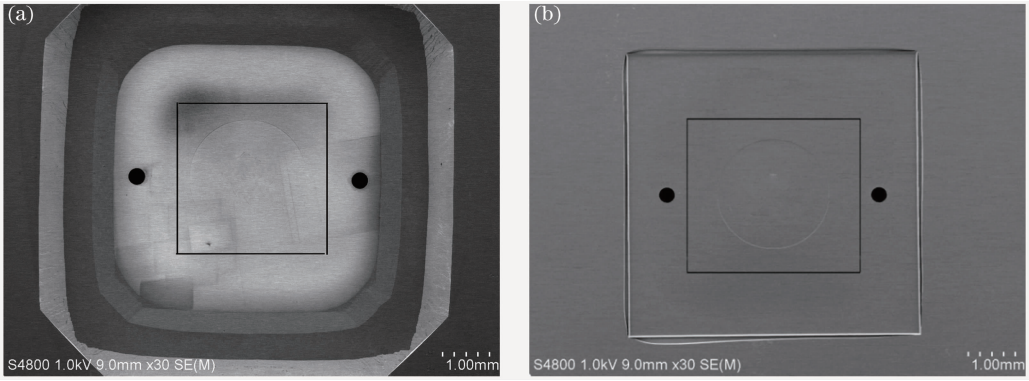

Fig. 9　MEMS sensitive diaphragm. (a) Elevation; (b) back elevation

When the radius of membrane and its thickness are 2.35 mm and 7 μm, using Eq. (2), the lowest self-oscillation frequency of flat membrane can be calculated. And without considering damping coefficient, the deformation equation of flat membrane forced vibration can be expressed as[12]

$$Y_0 = \frac{3p(1-\mu^2)r^4}{16Eh^3}\frac{f_0^2}{\sqrt{(f_0^2-f^2)^2}}, \qquad (11)$$

where f_0 is the lowest self-oscillation frequency of flat membrane, f is the frequency of the external pressure. The relationship between frequency of the external pressure f and deformation of flat membrane Y_0 can be seen in Fig. 10.

In order to ensure that the sensor has a relatively flat frequency response, the lowest self-oscillation frequency of flat membrane should be at least three times the maximum detectable frequency[16]. So the size of the flat membrane in this paper is suitable for testing

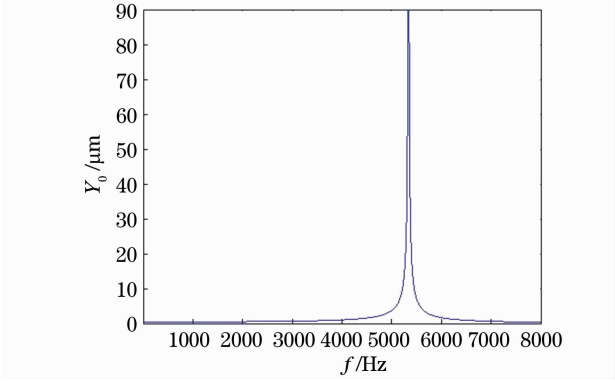

Fig. 10 Frequency response of flat membrane.

the low frequency less than 2 kHz.

The normalized coupling loss was measured as a ratio of the power (P) to the power transmitted with perfect alignment in the corresponding situation (P_0). The measured normalized coupling loss is denoted as

$$L_n = -10\lg(P/P_0). \tag{11}$$

The normalized coupling loss because of the change of distance between C-lens and flat diaphragm indicates the coupling loss that is due to the corresponding misalignment.

Figures 11 (a) and (b) show the test results in condition of acoustical signals (100 Hz, 5 Pa) and (50 Hz, 5 Pa), respectively. The receiver uses HFBR2416 photovoltaic module produced by Agilent Company (photoelectric conversion efficiency is 7.8 mV/μW).

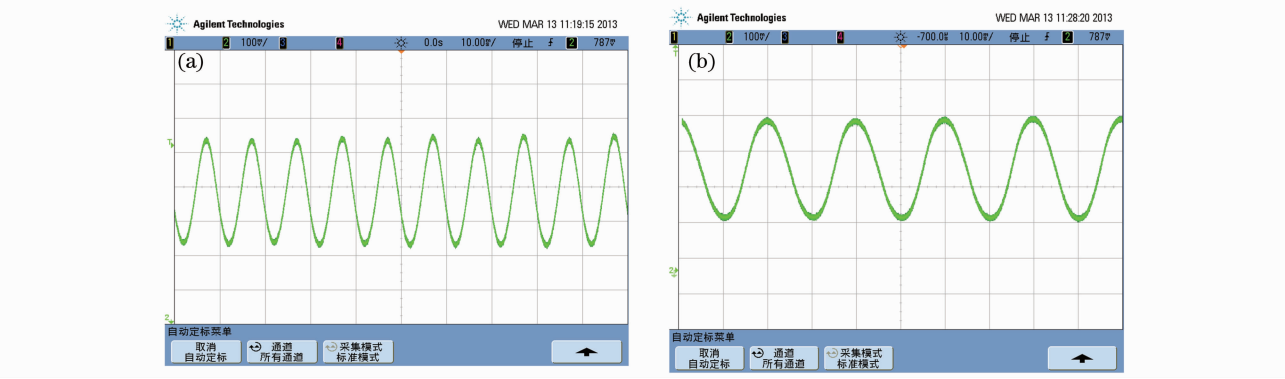

Fig. 11 Response of sensor to sound pressure level. (a) 10 Hz, 5 Pa; (b) 50 Hz, 5 Pa

Table 1 Experimental data

Pressure /Pa	Vibration displacement of membrane /μm	Average receiving optical power /μW
0	0	157.1
3.5	0.10	135.2
5.0	0.20	118.9
7.5	0.30	86.1
10.0	0.40	51.9
12.5	0.50	29.1
15.0	0.60	14.5

Acoustic waves were generated by a speaker driven by a signal generator; the acoustic signal frequency was 100 Hz. The values in Table 1 are the experimental results under different pressures. The reason why displacement vibration increases with the decrease in average receiving optical power is that with θ (tilt angle) in Fig. 1 increasing the coupling loss increases.

Figure 12 shows the normalized coupling loss that is due to different pressures acting on the flat membrane. When the pressure acting on sensor increases, the displacement of membrane increases, which leads to reflection light (the light will be reflected to C-lens) angular tilt change, and this change leads to optical coupling loss change. In this figure the

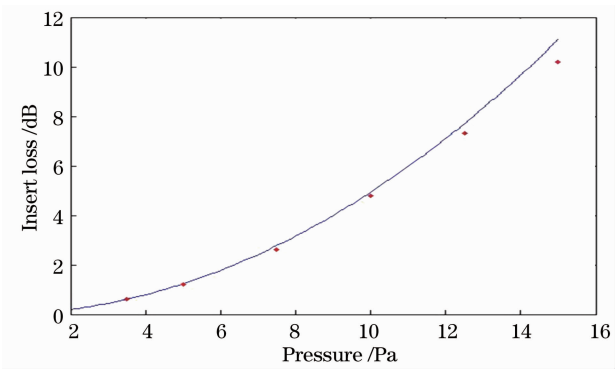

Fig. 12 Comparison of the experimental (dots) and theoretical (curve) results for the normalized coupling loss when flat membrane radius is 2.35 mm and thickness is 7 μm.

theoretical analysis agrees with the experimental results approximately.

6 Conclusion

We have presented a fiber-optic acoustic transducer incorporating a compact fiber collimator and a reflective MEMS diaphragm. And a general formula for the coupling loss with the existence of angular tilt misalignments has been used. The results indicate that the direct influence of this transducer is the change of MEMS membrane tilt angle. Other parameters like membrane thickness, membrane radius and sound pressure impact the transducer through making membrane tilt angle change. The tilt angle change is due to the vibration of membrane. We have also analyzed the detection sensitivity using different related parameters. Simulation and experimental results show that the algorithm proposed in this paper can make the sensitivity of the fiber-optic acoustic transducer improve in orders of magnitude than traditional methods[17]. For example, Fig. 6 shows that when the membrane displacement changes from 0.25 μm to 0.5 μm, the coupling loss changes from about 2 dB to 8 dB (from 63% to 16%). For the displacement vibration of 0.25 μm, the light intensity vibration is 47%. In comparison, for traditional methods, the corresponding values are about 200 μm and 20%, respectively.

References

1 R Li, N Madamopoulos, W Xiao. Influence of membrane surface shape change on the performance characteristics of a fiber optic microphone [J]. Appl Opt, 2010, 49(35): 6660 - 6667.

2 J P F Wooler, B Hodder, R I Crickmore. Acoustic properties of a fibre-laser microphone [J]. Meas Sci & Technol, 2007, 18(3): 884 - 888.

3 P McDowell, B Bourgeois, P J McDowell, *et al*.. Relative positioning for team robot navigation [J]. Autonomous Robots, 2007, 22(2): 133 - 148.

4 J Chambers, D Bullock, Y Kahana. Developments in active noise control sound systems for magnetic resonance imaging [J]. Appl Acoust, 2007, 68(3): 281 - 295.

5 J A Bucaro, N Lagakos, B H Houston. Miniature, high performance, low-cost fiber optic microphone [J]. Acoust Soc Am, 2005, 118(3): 1406 - 1413.

6 J Song, S Lee. Fiber-optic acoustic transducer utilizing a dual-core collimator combined with a reflective micromirror [J]. Microwave Opt Technol Lett, 2006, 48(9): 1833 - 1836.

7 J M S Sakamoto, G M Pacheco. Theory and experiment for single lens fiber optical microphone [J]. Physics Procedia, 2010, 3(1): 651 - 658.

8 Z H Ju, Y S Li, M Lei. Theoretical analysis of sensing probe in fiber microphone [J]. J Appl Opt, 2008, 29(5): 812 - 814.

9 K K Chin, Y Sun, G H Feng, *et al*.. Fabry-Perot diaphragm fiber-optic sensor [J]. Appl Opt, 2007, 46(31): 7614 - 7619.

10 R W Gilsdorf, J C Palais. Single-mode fiber coupling efficiency with graded-index rod lenses [J]. Appl Opt, 1994, 33(16): 3440 - 3445.

11 O Wallner, P J Winzer, W R Leeb. Alignment tolerances for plane-wave to single-mode fiber coupling and their mitigation by use of pigtailed collimators [J]. Appl Opt, 2002, 41(4): 637 - 643.

12 W Q Yun. Study on Fiber Optic Fabry-Perot Acoustic Sensor and Its Application [D]. Dalian: Dalian University of Technology, 2010.

13 H Kogelnik. Coupling and conversion coefficients for optical modes [C]. Proceedings of the Symposium on Quasi-Optics, 1964, 14: 335 - 347.

14 S Nemeto, T Makimoto. Analysis of splice loss in single-mode fibers using a Gaussian field approximation [J]. Opt Quantum Electron, 1979, 11(5): 447 - 457.

15 S F Yuan, A R Nabeel. General formula for coupling-loss characterization of single-mode fiber collimators by use of gradient-index rod lense [J]. Appl Opt, 1999, 38(15): 3214 - 3222.

16 Xu J. High Temperature High Bandwidth Fiber Optic Pressure Sensors [D]. Blacksburg: Virginia Polytechnic Institute and State University, 2005.

17 P B Buchade, A D Shaligram. Influence of fiber geometry on the performance of two-fiber displacement sensor [J]. Sensors and Actuators A, 2007, 136(1): 199 - 204.

栏目编辑：宋梅梅